Studies of densities and charge form factors of light, medium and heavy neutron-rich exotic nuclei

A. N. Antonov[1], D. N. Kadrev[1], M. K. Gaidarov[1], E. Moya de Guerra[2], P. Sarriguren[2], J. M. Udias[3], V. K. Lukyanov[4], E. V. Zemlyanaya[4], G. Z. Krumova[5]

[1]*Institute for Nuclear Research and Nuclear Energy, Sofia, Bulgaria*
[2]*Instituto de Estructura de la Materia, CSIC, Serrano 123, Madrid, Spain*
[3]*Universidad Complutense de Madrid, Madrid, Spain*
[4]*Joint Institute for Nuclear Research, Dubna, Russia*
[5]*University of Rousse, Rousse, Bulgaria*

I. Introduction

II. The Theoretical scheme

A. The Form Factors

B. The Density Distributions

III. Results and Discussion

IV. Conclusions

– A. N. Antonov, D. N. Kadrev, M. K. Gaidarov, E. Moya de Guerra, P. Sarriguren, J. M. Udias, V. K. Lukyanov, E. V. Zemlyanaya, G. Z. Krumova, nucl-th/0506056 (2005)
Phys. Rev. C **72** (2005), in print

I. Introduction

It has been found from analyses of total interaction cross sections (Tanihata et al.) that weakly-bound neutron-rich light nuclei, e.g. ^{6,8}He, ^{11}Li, ^{14}Be, ^{17,19}B, have increased sizes that deviate substantially from the $R \sim A^{1/3}$ rule.

It was realized (e.g. Hansen (1995), Dobaczewski (1994), Casten and Sherill (2000)) that such a new phenomenon is due to the weak binding of the last few nucleons which form a diffuse nuclear cloud due to quantum-mechanical penetration (the so called "nuclear halo").

Another effect is that the nucleons can form a "neutron skin" when the neutrons are on average less bound than the protons. The origin of the skin lies in the large difference of the Fermi energy levels of protons and neutrons so that the neutron wave function extends beyond the effectively more bound proton wave function. Thus, the term "neutron skin" describes an excess of neutrons at the nuclear surface, whereas the "halo" stands for such excess plus a long tail of the neutron density distribution.

The aim of this work is as follows.

Firstly, to extend the range of exotic nuclei for which charge form factors are calculated. Along with the new calculations for He and Li isotopes, we present results on charge form factors of several unstable isotopes of medium (Ni) and heavy (Kr and Sn) nuclei and compare them to those of stable isotopes in the same isotopic chain. The isotopes of Ni and Sn are chosen because they have been indicated as first candidates accessible for the charge densities and rms radii determination and as key isotopes for structure studies of unstable nuclei at the electron-radioactive-ion collider in RIKEN.

We also give the charge densities and compare them to matter density distributions.

We calculate the charge form factors not only within the PWBA but also in DWBA by the numerical solution of the Dirac equation for electron scattering in the Coulomb potential of the charge distribution of a given nucleus.

Also, now we do not neglect the charge distribution in the neutrons themselves.

II. The Theoretical Scheme

A. The Form Factors

In Born approximation the charge form factor is:

$$F_{ch}(q) = \frac{1}{\int \rho_{ch}(\mathbf{r})d\mathbf{r}} \int \rho_{ch}(\mathbf{r}) e^{\mathbf{iqr}} d\mathbf{r}. \tag{1}$$

The total charge distribution:

$$\rho_{ch}(\mathbf{r}) = \rho_{ch}^{(p)}(\mathbf{r}) + \rho_{ch}^{(n)}(\mathbf{r}) \tag{2}$$

Proton part of total charge distribution:

$$\rho_{ch}^{(p)}(\mathbf{r}) = \int \rho_{point,p}(\mathbf{r} - \mathbf{r}')\rho_p(\mathbf{r}')d\mathbf{r}'. \tag{3}$$

Neutron part of total charge distribution:

$$\rho_{ch}^{(n)}(\mathbf{r}) = \int \rho_{point,n}(\mathbf{r} - \mathbf{r}')\rho_n(\mathbf{r}')d\mathbf{r}'. \tag{4}$$

Accounting for the c.m. correction $F_{c.m.}(q) = \exp(q^2/4A^{2/3})$, we finally obtain:

$$F_{ch}(q) = \left[F_{point,p}(q)G_{Ep}(q) + \frac{N}{Z}F_{point,n}(q)G_{En}(q)\right]F_{c.m.}(q), \qquad (1)$$

where $F_{ch}(0) = 1$, because $G_{En}(0) = 0$ and $G_{Ep}(0) = 1$; $F_{point,p}(0) = 1$ and $F_{point,n}(0) = 1$; G_{En} and G_{Ep} are the Sachs proton and neutron electric form factors, and

$$F_{point,p}(\mathbf{q}) = \frac{1}{Z}\int \rho_{point,p}(\mathbf{r})e^{i\mathbf{qr}}d\mathbf{r} \qquad (2)$$

$$F_{point,n}(\mathbf{q}) = \frac{1}{N}\int \rho_{point,n}(\mathbf{r})e^{i\mathbf{qr}}d\mathbf{r}, \qquad (3)$$

where

$$\int \rho_{point,p}(\mathbf{r})d\mathbf{r} = Z; \qquad \int \rho_{point,n}(\mathbf{r})d\mathbf{r} = N. \qquad (4)$$

B. The Density Distributions

– ^{4,6,8}He ^{6,11}Li from the LSSM calculations [Karataglidis (1997,2000)]

– The point proton and neutron density distributions of Ni, Kr and Sn isotopes are taken from deformed self-consistent HFB calculations with density-dependent SG2 effective interactions using a large HO basis with 11 major shells.

III. Results and Discussions

– point proton densities

– matter densities

$$\rho_m(r) = \rho_{point,p}(r) + \rho_{point,n}(r)$$

– proton, neutron, charge and matter rms radii

– diffuseness parameter values

– charge form factors

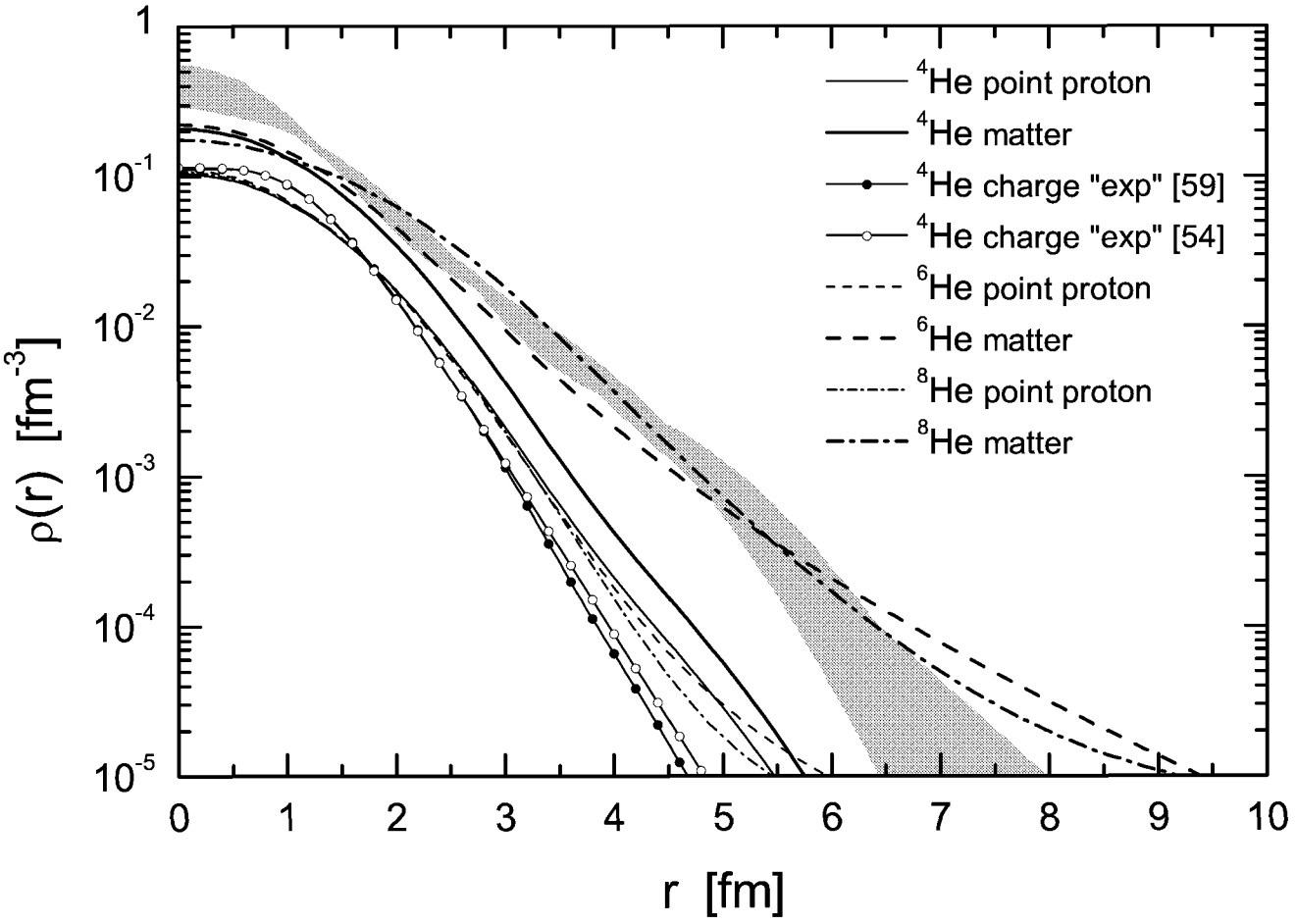

Figure 1: Thin lines are LSSM point proton densities of ^{4,6,8}He compared to the "experimental" charge density for ^{4}He from "model-independent" analyses [54] Burov (1977,1998), [59] De Vries (1987). Thick lines are LSSM matter densities of ^{4,6,8}He compared to matter density of ^{8}He deduced from the experimental proton scattering cross section data of Egelhof (2003) (grey area).

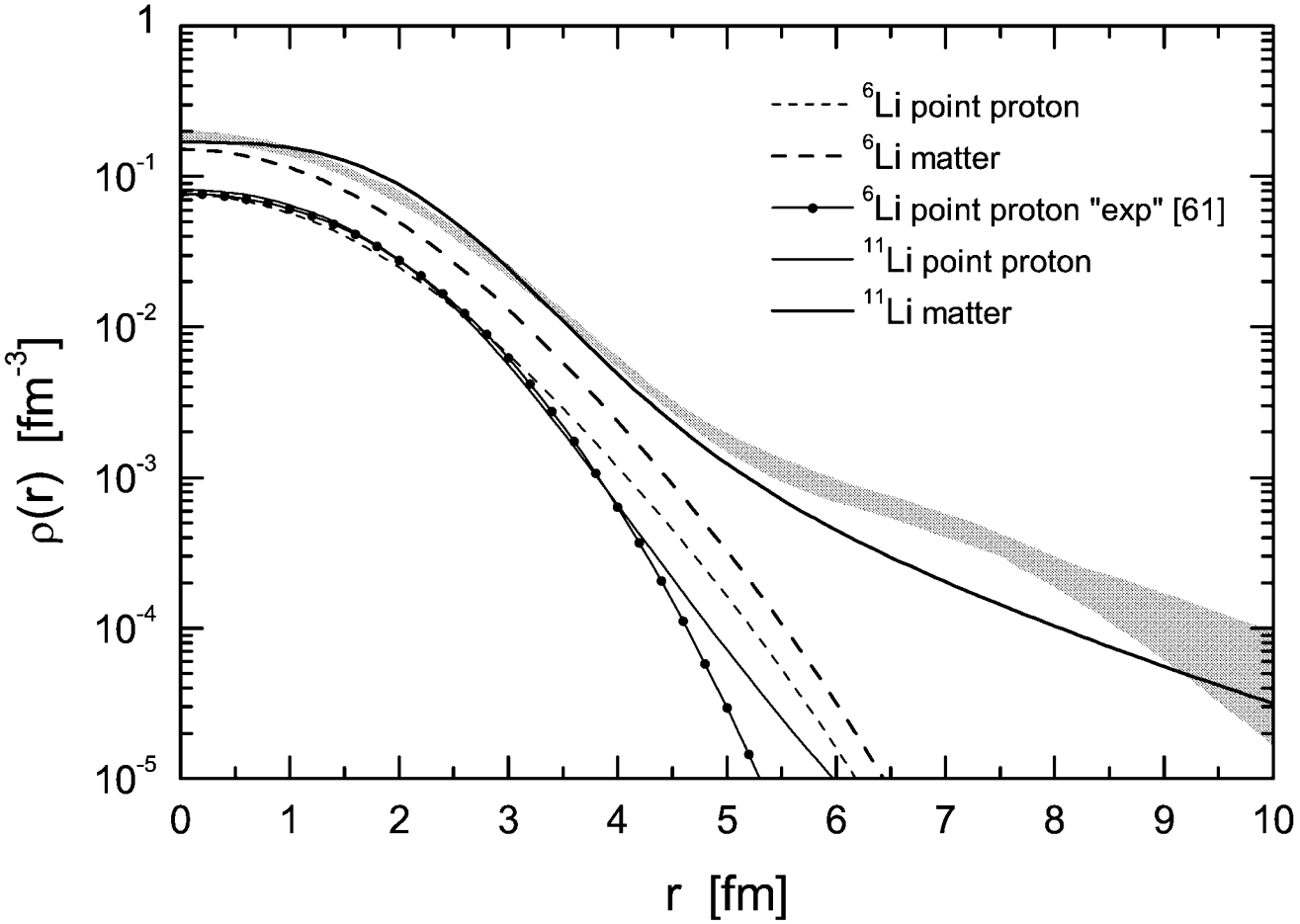

Figure 2: Thin lines are LSSM point proton densities of ^{6,11}Li compared to the point-proton density of ^{6}Li extracted from the "experimental" charge density in a "model-independent" analysis [61] Patterson (2003). Thick lines are LSSM matter densities of ^{6,11}Li compared to matter density of ^{11}Li deduced from the experimental proton scattering cross section data of Egelhof (2003) (grey area).

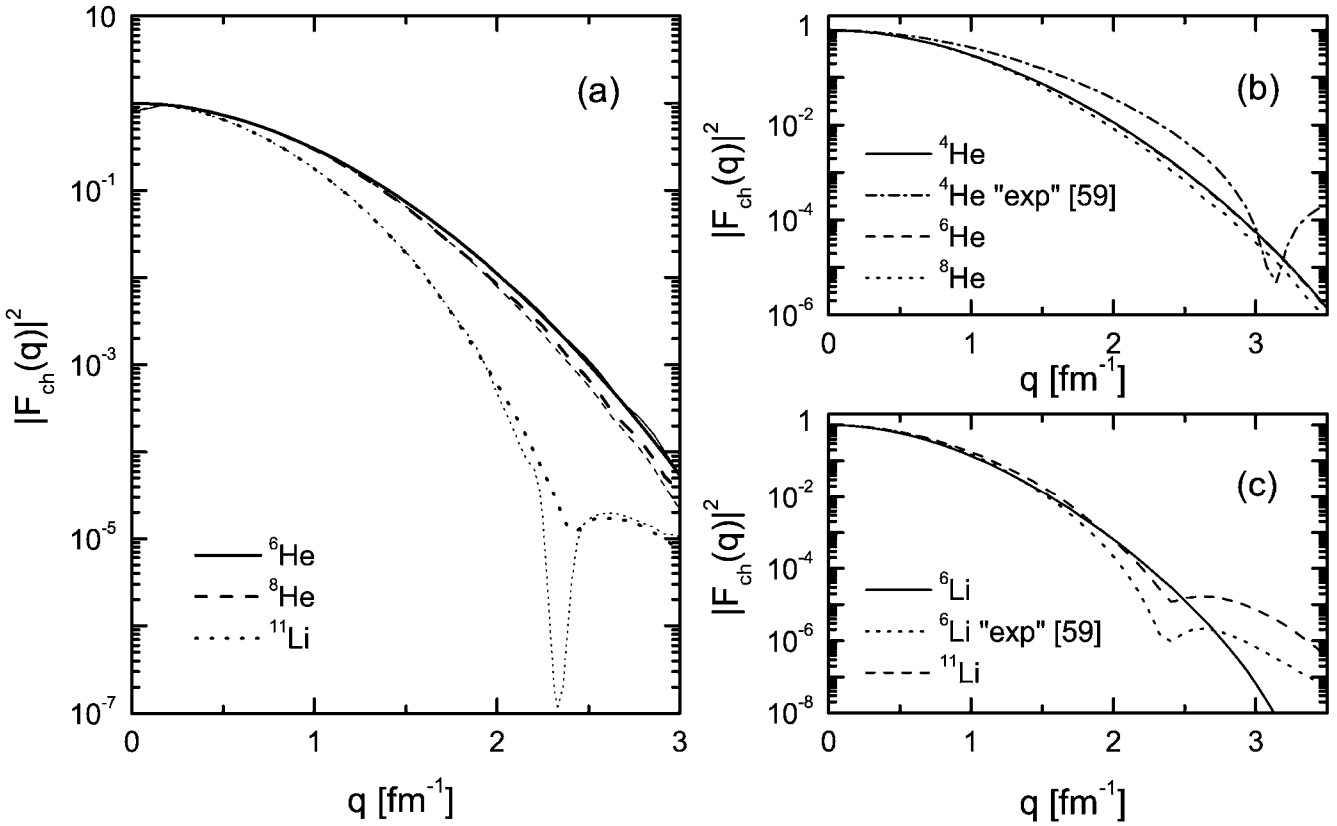

Figure 3: (a) Charge form factors of ^{6}He, ^{8}He and ^{11}Li calculated in PWBA (thin lines) and in DWBA (thick lines) using LSSM densities; (b) charge form factors in DWBA for ^{4}He (calculated by using "experimental" charge density [59] De Vries (1987) and the LSSM density) and of ^{6,8}He (using the LSSM densities); (c) charge form factor in DWBA for ^{6}Li (using the "experimental" charge density [59] De Vries (1987) and the LSSM densities) and for ^{11}Li (using the LSSM densities).

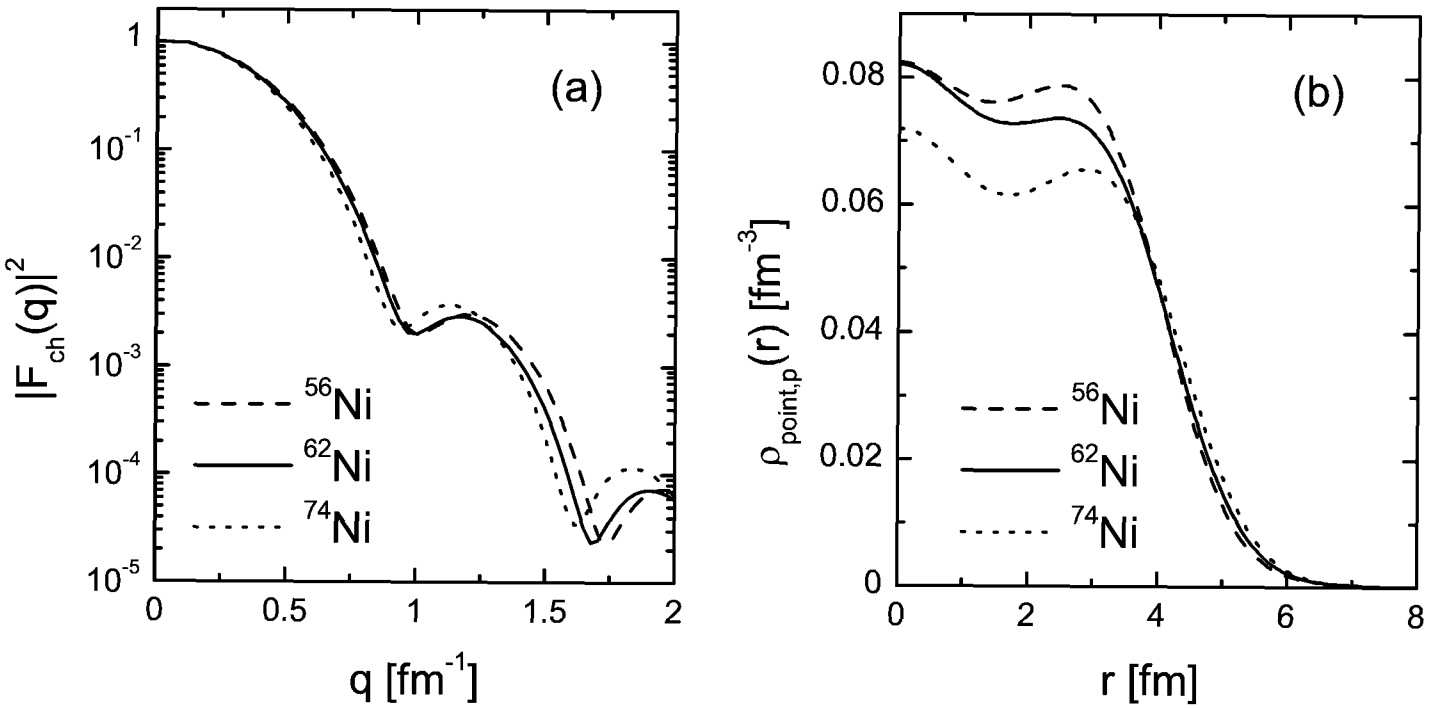

Figure 4: (a) Charge form factors for the unstable doubly-magic ^{56}Ni, stable ^{62}Ni and unstable ^{74}Ni isotopes calculated by using the HF+BCS densities and the DWBA; (b) HF+BCS proton densities of ^{56}Ni, ^{62}Ni and ^{74}Ni.

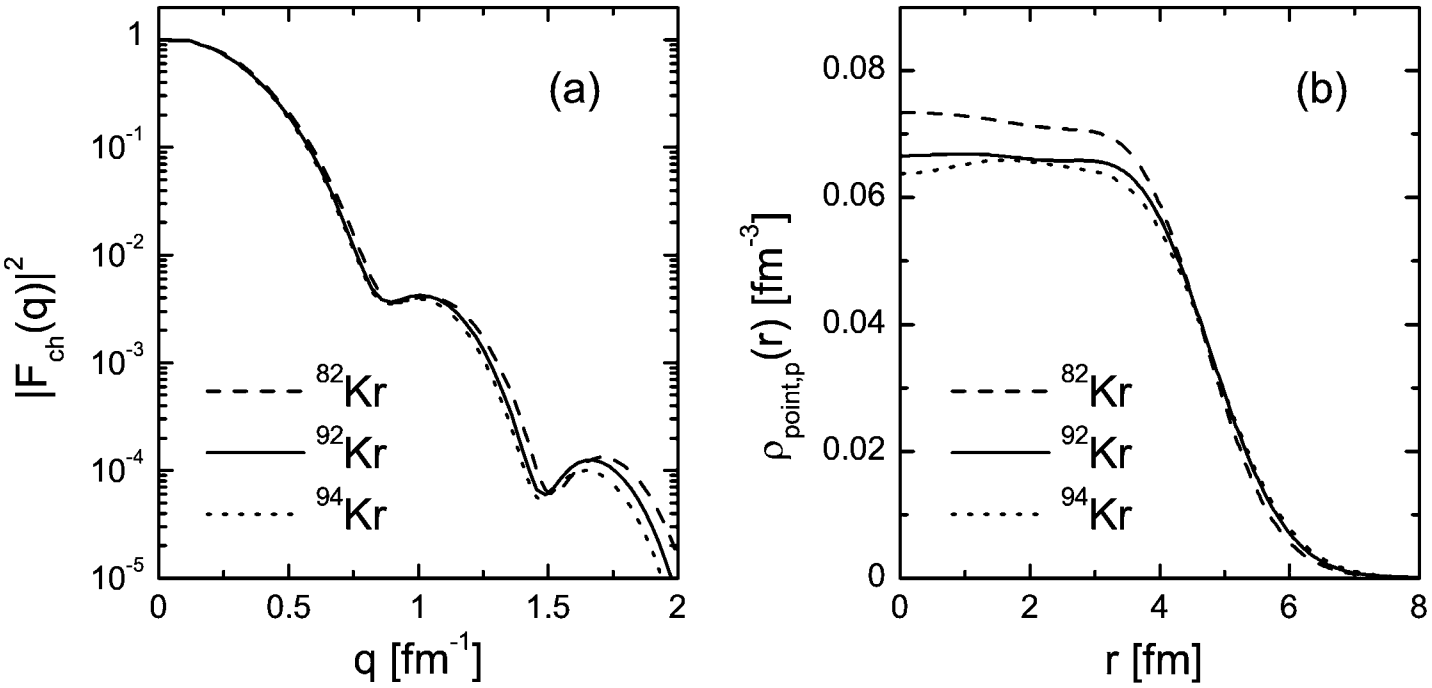

Figure 5: (a) Charge form factors for the stable isotope ^{82}Kr and for the unstable ^{92}Kr and ^{94}Kr isotopes calculated by using the HF+BCS densities and the DWBA; (b) HF+BCS proton densities of ^{82}Kr, ^{92}Kr and ^{94}Kr.

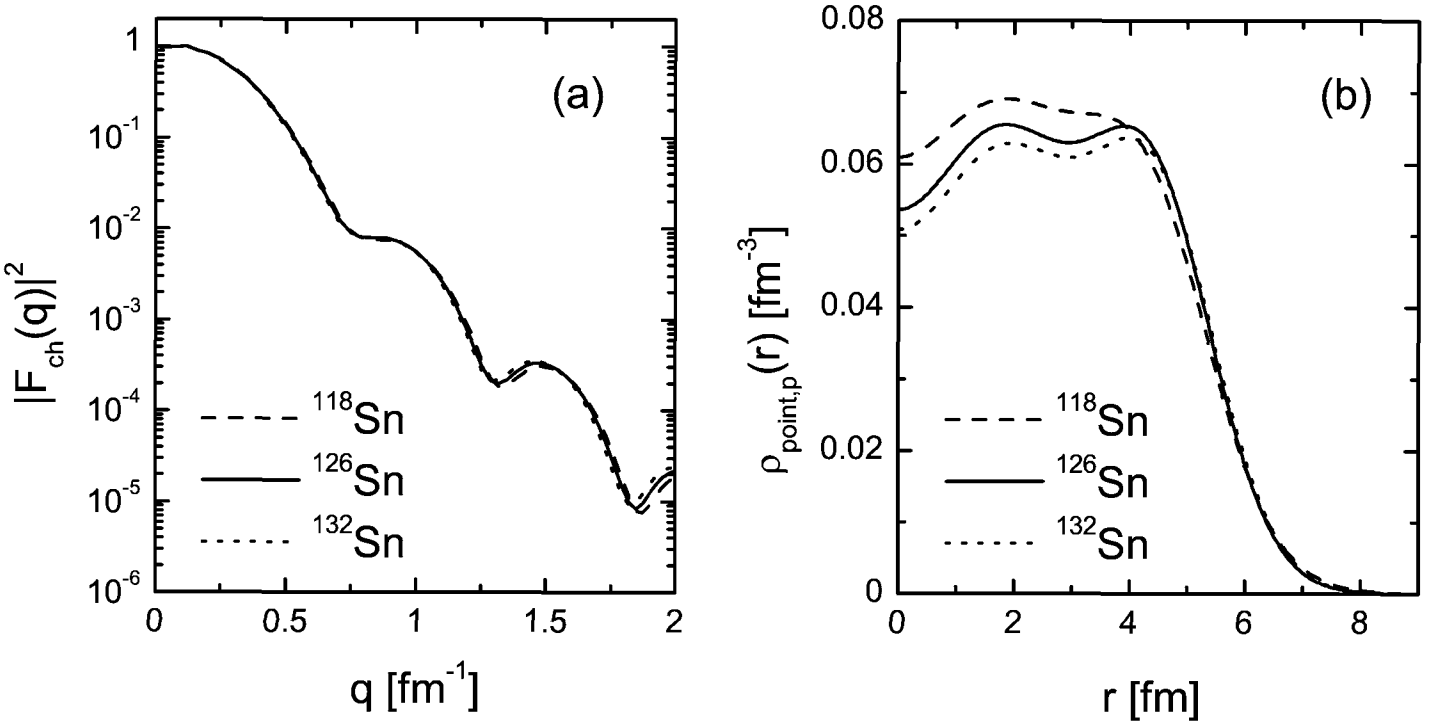

Figure 6: (a) Charge form factors for the stable isotope ^{118}Sn, unstable ^{126}Sn and unstable doubly-magic ^{132}Sn isotopes calculated by using the HF+BCS densities and the DWBA; (b) HF+BCS proton densities of ^{118}Sn, ^{126}Sn and ^{132}Sn.

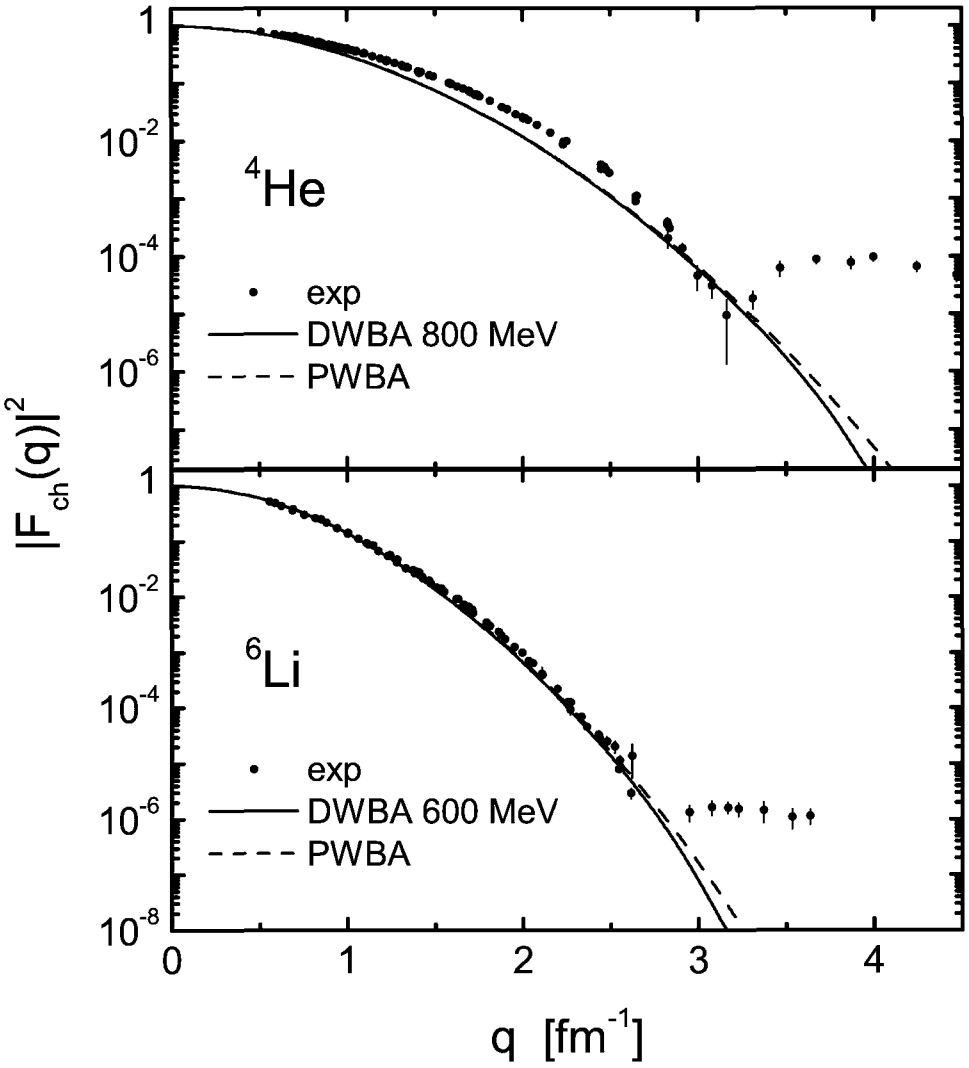

Figure 7: Charge form factors for the stable isotopes ^{4}He and ^{6}Li calculated using LSSM densities in PWBA and in DWBA in comparison with the experimental data.

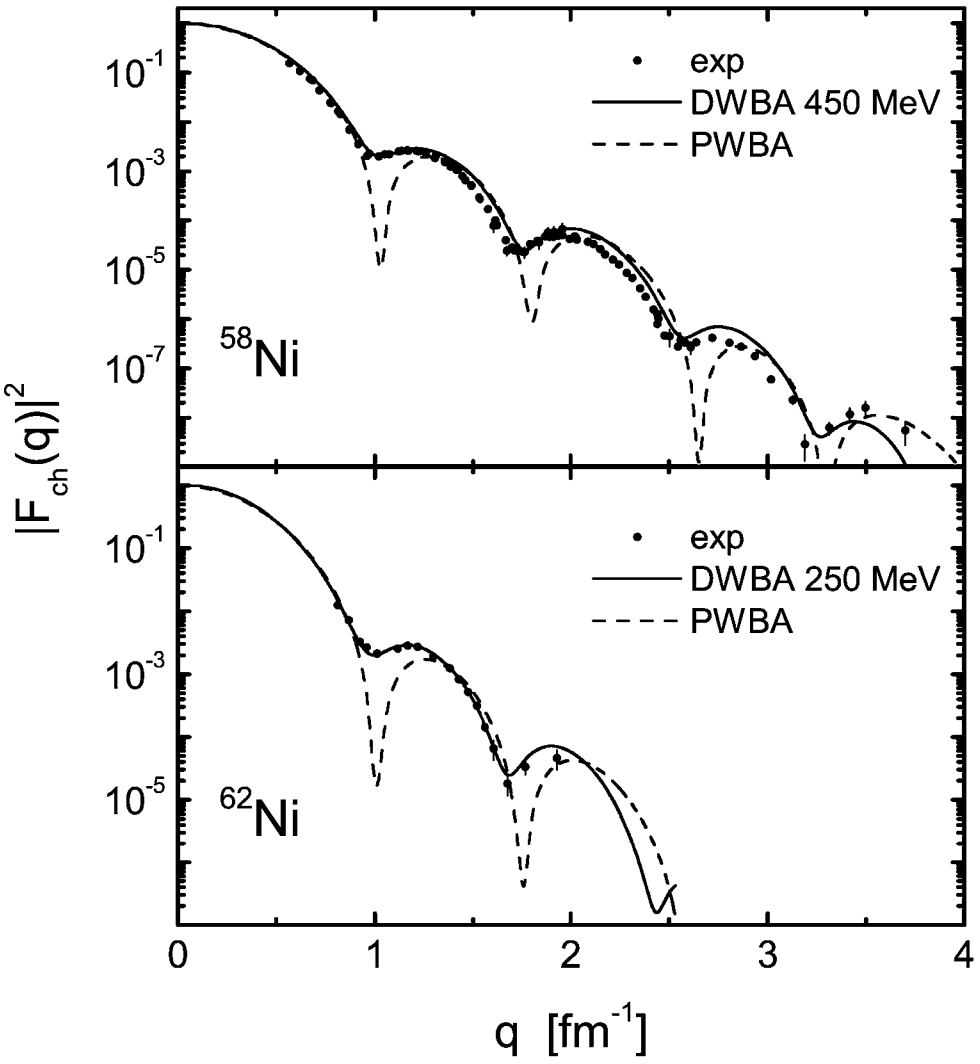

Figure 8: Charge form factors for the stable isotopes ^{58}Ni and ^{62}Ni calculated by using the HF+BCS densities and the PWBA and DWBA in comparison with the experimental data.

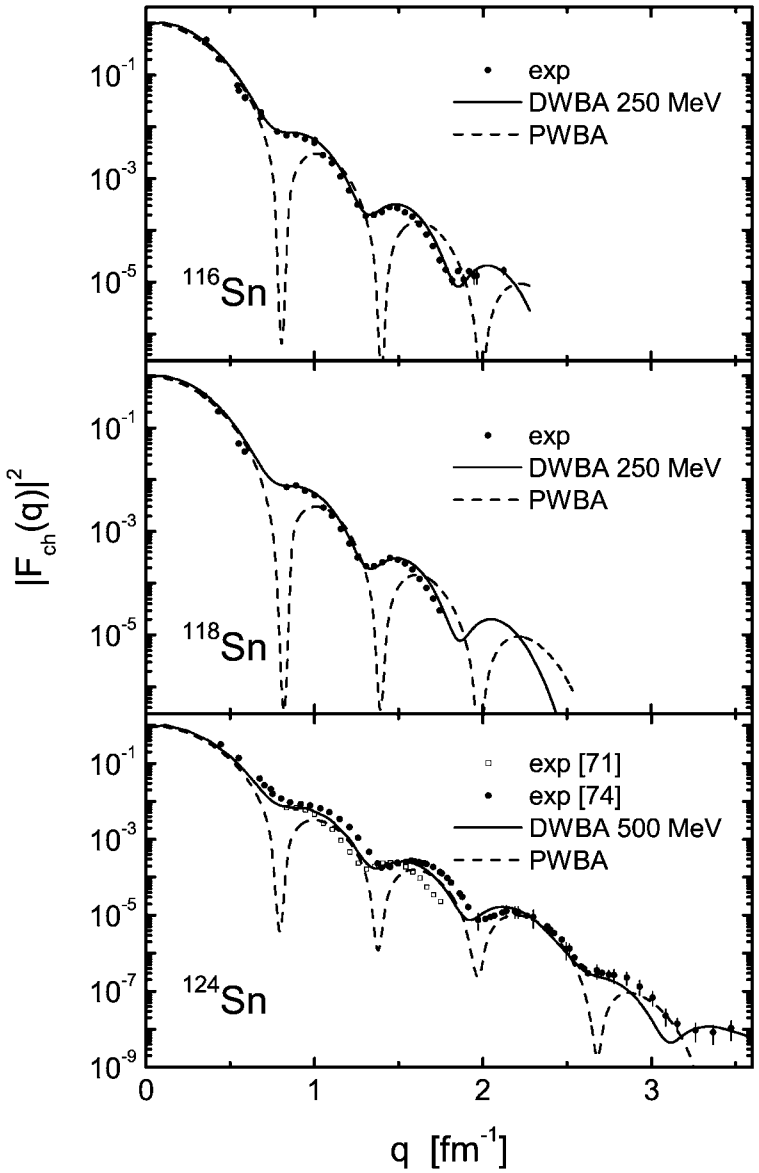

Figure 9: Charge form factors for the stable isotopes ^{116}Sn, ^{118}Sn and ^{124}Sn calculated by using the HF+BCS densities and the PWBA and DWBA in comparison with the experimental data [71] Litvinenko (1972), [74] Cavedon (1982).

$$F_{ch}(q) = \left[F_{point,p}(q) G_{Ep}(q) + \frac{N}{Z} F_{point,n}(q) G_{En}(q) \right] F_{c.m.}(q) \qquad (1)$$

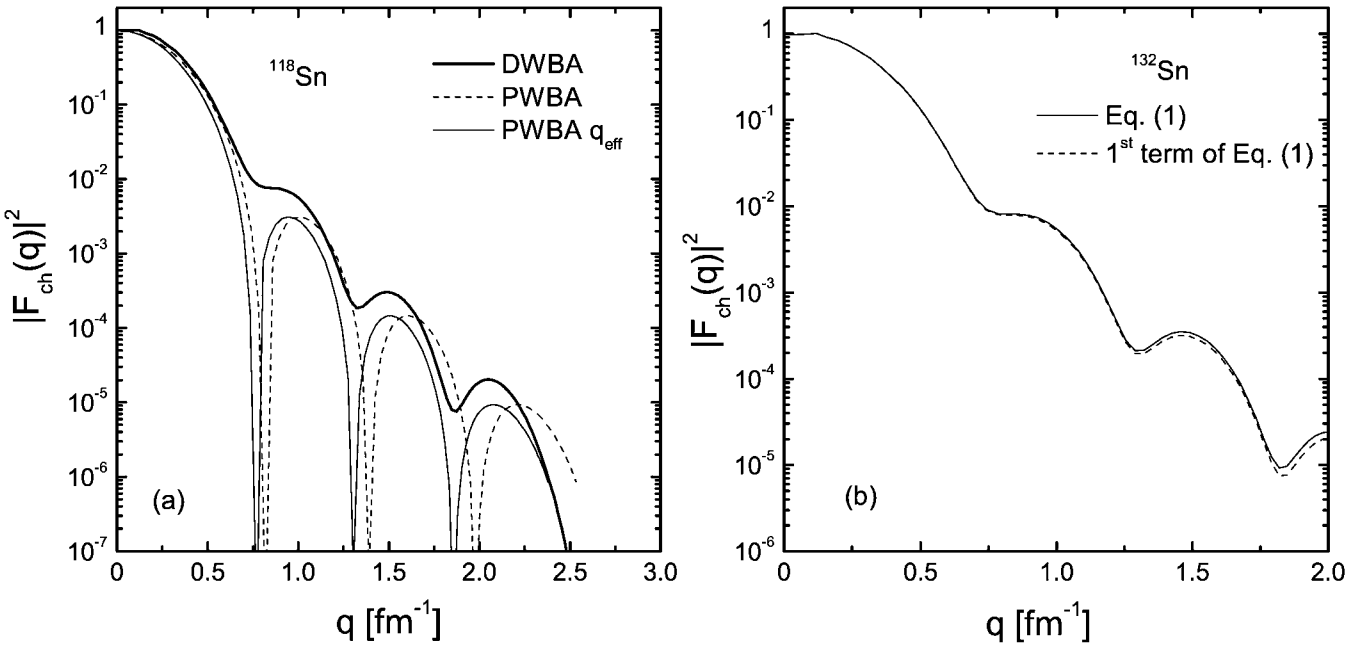

Figure 10: (a) Charge form factors for the stable isotope ^{118}Sn calculated by using the DWBA (thick solid line), PWBA (dashed line) and PWIA with $q_{eff} = q[1 + (cZ\alpha/R_{ch}E_i)]$, $c = 1$ (thin solid line); (b) Charge form factor for the unstable doubly-magic ^{132}Sn isotope calculated by using the DWBA and corresponding to Eq. (1) (solid line) and to the proton contribution only [i.e. to the first term of Eq. (1)] (dashed line).

TABLE I: Proton (R_p), neutron (R_n), charge (R_{ch}), matter (R_m) rms radii (in fm) and difference $\Delta R = R_m - R_p$ of He and Li isotopes calculated using LSSM densities. Available data on R_m and R_{ch} are also presented.

Nuclei	R_p	R_n	R_{ch}	R_m	ΔR	R_m [1]	R_m [2,3]	R_m [4,5]	R_{ch} [6,7]	R_{ch} [8]
^{4}He	1.927	1.927	2.153	1.927	0.000	1.49(3)			1.696(14)	1.695
^{6}He	1.945	2.900	2.147	2.621	0.676	2.30(7)	2.33(4)	2.54(4)		
^{8}He	1.924	2.876	2.140	2.670	0.746	2.45(7)	2.49(4)			
^{6}Li	2.431	2.431	2.647	2.431	0.000	2.45(7)	2.32(3)		2.57(10)	2.539
^{11}Li	2.238	3.169	2.477	2.945	0.707	3.62(19)	3.12(16)	3.53(10)		

[1] Egelhof (2002); [2,3] Tanihata (1988,1992); [4,5] Tostevin (1996,1997); [6] De Vries (1987); [7] Patterson (2003); [8] Burov (1977,1998)

TABLE II: Proton (R_p), neutron (R_n), charge (R_{ch}), matter (R_m) rms radii (in fm) and difference $\Delta R = R_m - R_p$ of Ni, Kr and Sn isotopes calculated using HF+BCS densities. The last two columns present experimental data on R_{ch}.

Nuclei	R_p	R_n	R_{ch}	R_m	ΔR	R_{ch} [1]	R_{ch} [2]
^{56}Ni	3.725	3.666	3.795	3.696	-0.029		
^{58}Ni	3.719	3.697	3.794	3.707	-0.012	3.764(10)	
^{62}Ni	3.798	3.855	3.866	3.829	0.031	3.830(13)	
^{74}Ni	3.911	4.130	3.977	4.049	0.138		
^{82}Kr	4.126	4.190	4.189	4.162	0.036		4.192(4)
^{92}Kr	4.224	4.412	4.285	4.340	0.116		4.273(16)
^{94}Kr	4.277	4.496	4.338	4.413	0.136		4.300(20)
^{116}Sn	4.583	4.650	4.646	4.621	0.038	4.626(15)	
^{118}Sn	4.649	4.739	4.705	4.701	0.052	4.679(16)	
^{126}Sn	4.642	4.798	4.698	4.737	0.095		
^{132}Sn	4.685	4.879	4.740	4.807	0.122		

[1] Patterson (2003); [2] Keim (1995)

TABLE III: Diffuseness parameter values (in fm) of the LSSM densities of He and Li isotopes and HF+BCS densities of Ni, Kr and Sn isotopes considered in this work.

Nuclei	a_p	a_n	a_m	a_{ch}
^{4}He	0.407	0.407	0.407	0.392
^{6}He	0.397	0.498	0.448	0.381
^{8}He	0.403	0.513	0.549	0.387
^{6}Li	0.521	0.521	0.521	0.509
^{11}Li	0.482	0.444	0.493	0.478
^{56}Ni	0.484	0.505	0.493	0.527
^{62}Ni	0.920	0.557	0.572	0.616
^{74}Ni	0.538	0.445	0.475	0.552
^{82}Kr	0.509	0.459	0.477	0.570
^{92}Kr	0.505	0.541	0.527	0.564
^{94}Kr	0.516	0.761	0.639	0.582
^{118}Sn	0.468	0.555	0.509	0.534
^{126}Sn	0.382	0.707	0.482	0.445
^{132}Sn	0.377	0.698	0.473	0.434

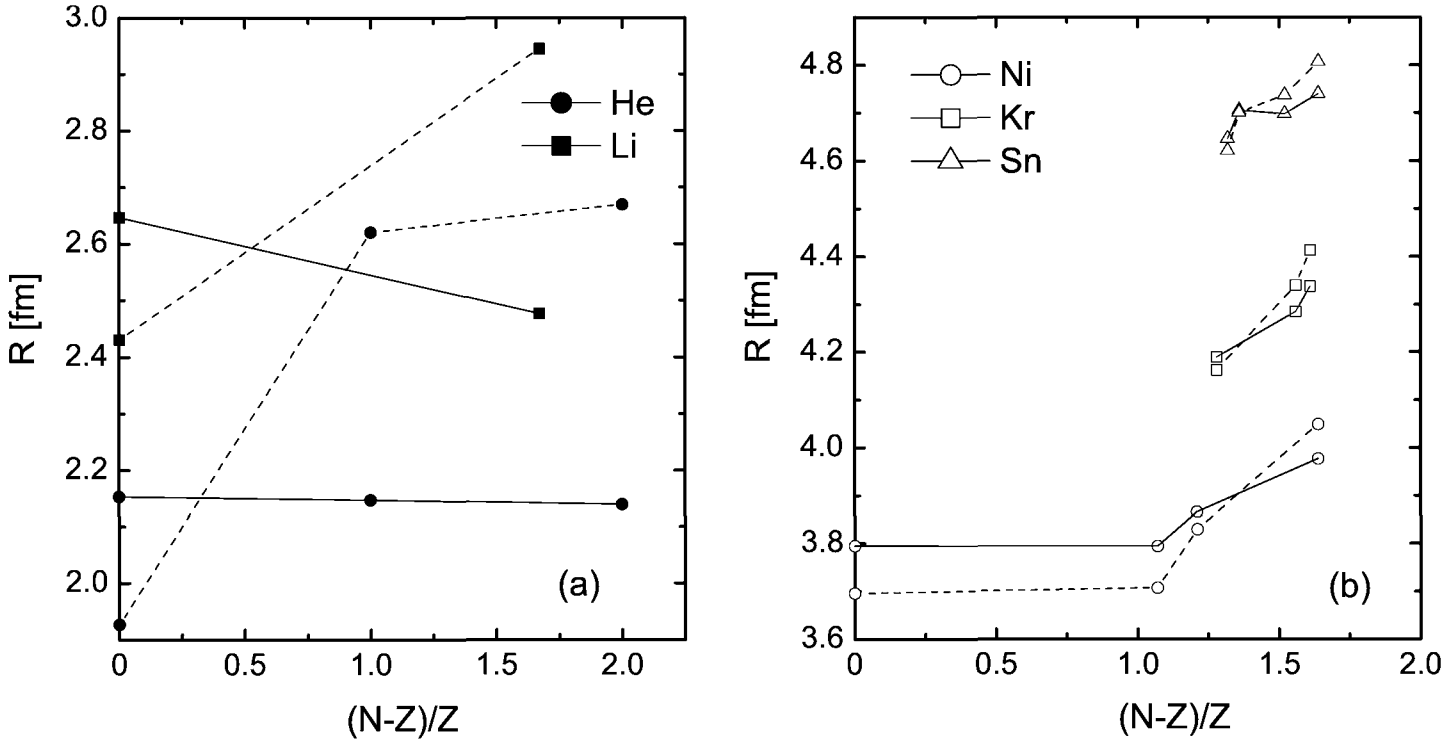

Figure 11: Charge (R_{ch}) (solid eye-guide lines) and matter (R_m) (dashed lines) rms radii calculated in this work as a function of the relative neutron excess $(N-Z)/Z$ of He and Li isotopes (full symbols) (a) and Ni, Kr and Sn isotopes (open symbols) (b).

$$R_{ch}^2 = -6 \left[\frac{dF_{ch}(q^2)}{d(q^2)} \right]_{q^2=0} \tag{1}$$

IV. Conclusions

1) In this work we extended the studies of the proton, neutron, charge and matter densities and related charge form factors from the light neutron-rich exotic nuclei ^{6,8}He, ^{11}Li to examples of unstable medium (Ni) and heavy (Kr and Sn) isotopes in comparison with those of stable isotopes in the same isotopic chain. For He and Li isotopes we use the proton and neutron densities obtained from realistic microscopic calculations within the large-scale shell-model method. The densities of Ni, Kr and Sn isotopes are calculated in HF+BCS method with a density-dependent effective interaction using a large harmonic-oscillator basis.

2) We also compare proton and matter density distributions for He and Li isotopes. The calculated matter distributions for the halo nuclei are much more extended than the proton ones. We compare proton density distributions for the isotopes of He, Li, Ni, Kr and Sn and establish the differences of the proton densities in a given isotopic chain due to the presence of the neutron excess. There is a decrease of the proton density in the nuclear interior and an increase of its tail at large r with increasing neutron number.

3) A comparison of the proton, neutron, charge and matter rms radii as well as the corresponding diffuseness is performed for all isotopic chains considered. We point out that the general trend of the difference ΔR between the matter and proton rms radii is to increase with the number of neutrons but for the heavy isotopes this increase is moderate compared to that of the light ones.

4) The calculated matter densities for ^{8}He and ^{11}Li are in fair agreement with the experimental data obtained in proton scattering on these isotopes in GSI (Egelhof). We compare the matter rms radii with those from GSI as well as with those from total interaction cross section data (Tanihata) and their re-analysis (Tostevin).

5) We calculate the charge form factors of He, Li, Ni, Kr and Sn isotopes by means of the densities mentioned above. The charge form factors are calculated not only in the PWBA but also in the DWBA, solving the Dirac equation for electron scattering in the Coulomb potential of the charge distribution in a given nucleus. By accounting for the Coulomb distortion of the electron waves the Born zeroes are filled and the form factors are shifted to smaller values of q which is clearly seen in the cases of the Ni, Kr and Sn isotopes where Z is large enough. We find that this shift is best parametrized by $q_{eff} = q[1+(Z\alpha/R_{ch}E_i)]$, where R_{ch} are the charge rms radii as given in the Tables. In addition we also take into account the charge distribution in the neutron itself. We find that the contributions from the neutrons to the charge form factors are less than 20 % up to $q \sim 2$ fm^{-1}.

6) The differences between the charge form factors in a given isotopic chain are shown. The common feature of the charge form factors is the shift of the form factor curves and their minima to smaller values of q with the increase of the neutron number in a given isotopic chain.This is due to the corresponding enhancement of the proton tails in the peripherical region of the nuclei.

7) The performed theoretical analyses of the densities and charge form factors can be a step in the studies of the influence of the increasing neutron number on the proton and charge distributions in a given isotopic chain. This is important for understanding the neutron-proton interaction in the nuclear medium. We emphasize also the questions of interest, namely, the necessary both kinematical regions of the proposed experiments and precision to measure small shifts in the form factors.

The theoretical predictions for the charge form factors of exotic nuclei are a challenge for their measurements in the future experiments in GSI and RIKEN and thus, for obtaining detailed information on the charge distributions of such nuclei. The comparison of the calculated charge form factors with the future data will be a test of the corresponding theoretical models used for studies of the exotic nuclei structure.